

## MODELING OF DECOMPOSITION AND SULPHATION OF OIL SHALE CARBONATES ON THE BASIS OF NATURAL LIMESTONE\*

A. TRIKKEL<sup>(1)</sup>, R. KUUSIK<sup>(2)\*\*</sup>

Tallinn Technical University,

<sup>(1)</sup> Department of Inorganic Chemistry

<sup>(2)</sup> Department of Chemical Engineering

5 Ehitajate Rd., 19086 Tallinn, Estonia

*Estonian oil shale is characterized by a high content of inorganic matter, calcium carbonate making up 57–75% of the total inorganic part. At combustion temperature the carbonates decompose, and the formed free oxides bind at pulverized firing about 80–85% of SO<sub>2</sub> formed during combustion already in the boiler. At fluidized-bed combustion the conditions for SO<sub>2</sub> binding are close to optimum, and nearly full capture of SO<sub>2</sub> is expectable. Modeling of oxide formation and SO<sub>2</sub> binding was the task of the present work.*

*In order to obtain data for mathematical modeling of the decomposition and sulphation processes of oil shale carbonaceous part, series of thermogravimetric experiments accompanied by X-ray and SEM analysis, specific surface and porosity measurements were carried out with some natural limestone samples.*

*Mathematically, the calcination process of limestone samples was satisfactorily described using a random pore distribution model, assuming that only chemical reaction limited the overall decomposition process. An extended unreacted shrinking core model with variable (conversion-dependent) effective diffusivity was applied to the sulphation data. From model calculations the kinetic parameters of the decomposition and binding reactions were determined.*

### Introduction

The major component of oil shale (OS) inorganic part is calcium carbonate, which makes up 57–75% of the total inorganic part. The dolomite content is about 5%, and the ratio of carbonates to terrigenous part which consists of fine-grained quartz, orthoclase, mica, marcasite and some hydromica is in the range of 1.5–3.8 [1, 2]. During OS combustion, sulphur present in the

---

\* Presented at Symposium on Oil Shale in Tallinn, Estonia, November 18–21, 2002.

\*\* Corresponding author: e-mail [rkuusik@edu.ttu.ee](mailto:rkuusik@edu.ttu.ee)

amount of 1.5–1.6% is released mainly in the form of  $\text{SO}_2$ . At pulverized firing about 80–85% of  $\text{SO}_2$  is bound already in the boiler by CaO and MgO formed in the decomposition process of carbonates. To improve  $\text{SO}_2$  removal, in-duct injection of sorbents (limestone or dolomite) is widely used in coal firing. Recycling of oil shale ash, which still contains about 15–25% of free CaO as free CaO or/and  $\text{Ca}(\text{OH})_2$ , can also be used [3–5].

For mathematical modeling of limestone decomposition and sulphation, several models have been proposed, like “unreacted shrinking core” (USC) and “uniform conversion” (UC) models [6–8], which can be correctly applied in specific cases. The USC model for constant-size particles [6] can be used for the first characterization of solid-gas reactions. However, this model is limited to the case where either kinetics or intraparticle diffusion is rate-determining, and chemically identical solids with different structure (porosity, pores surface area) cannot be distinguished.

In the present paper a “random pore distribution” (RP) model [9, 10] was used to derive kinetic parameters for limestone decomposition. This model has also been proposed to describe sulphation processes of limestone or lime, including free lime in oil shale ash [11]. Shortcoming of the RP model as well as of the “grain model” proposed by Szekely and Evans [12] is that changing structure of the solid during the reaction is not accounted for. In the process of sulphation of limestone or lime, the product layer consisting of  $\text{CaSO}_4$  is formed, and its volume noticeably exceeds the volume of the initial CaO or  $\text{CaCO}_3$ . So, to take into account the changing volume of the product layer, an extended USC model with variable diffusivity [13–16] was used to determine rate parameters on reaction kinetics, mass transfer and diffusion.

## Materials and Methods

In order to study the decomposition and sulphation processes of oil shale carbonaceous part and to obtain data for mathematical modeling of these processes, series of thermogravimetric (TG) experiments accompanied by X-ray and SEM analysis, specific surface area (SSA) and porosity measurements were carried out with a selection of natural limestone samples of various crystalline structure. Relatively pure minerals (low values of insoluble in hydrochloric acid residue (I.Res.)) and those with a high additive ( $\text{SiO}_2$ ,  $\text{Fe}_2\text{O}_3$ ,  $\text{Al}_2\text{O}_3$ ) content were chosen to achieve a certain variety in their SSA and its changes during decarbonization (Table 1).

TG experiments of decarbonization were carried out using a derivatograph and the following experiment conditions: dynamic heating 10 K/min; sample weight 200 mg; particle size 125–160  $\mu\text{m}$ ;  $\text{CO}_2$  concentration in air 0, 15 or 100% with a gas flow rate 30 L/h; plate-type crucibles. In the experiments of sulphation a pressurized TG device (isothermal heating at 850 °C; 50 mg of sample diluted with 250 mg of quartz; particle size 125–

160  $\mu\text{m}$ ; gas composition 4%  $\text{O}_2$ , 15%  $\text{CO}_2$ , 0.5%  $\text{SO}_2$  and the rest of  $\text{N}_2$ ; gas flow rate 1.5 L/min; pressure 1 or 15 bar; specific sample-holders to diminish sample-bed and external diffusion) was used. Porosity measurements were carried out by the high-pressure Hg intrusion method, SSA measurements by nitrogen adsorption method.

Limestone decomposition and sulphation were characterized by the conversion level ( $X$ ),  $\text{SO}_2$  binding by both the amount of  $\text{SO}_2$  bound by 100 mg of initial sample ( $BC$ ,  $\text{mgSO}_2/100$  mg sample) and binding rate ( $W$ ,  $\text{mgSO}_2/100$  mg sample per second).

Table 1. Characterization of the Limestone Samples

Sample	SSA, $\text{m}^2/\text{g}$		Content, %						
	initial	calcined*	$\text{CO}_2$	CaO	$\text{CaCO}_3$	$\text{MgCO}_3$	I. Res.	$\text{Fe}_2\text{O}_3$	$\text{Al}_2\text{O}_3$
L04	4.58	4.56	34.12	44.56	75.29	1.95	10.38	0.68	10.20
L11	1.14	10.00	40.78	52.64	88.75	3.37	4.20	0.34	0.16
L12	13.17	4.18	31.83	44.95	70.75	1.38	5.28	8.34	1.88
L14	4.15	4.85	33.80	44.85	74.14	2.30	14.38	0.73	0.84
L22	0.87	15.48	42.12	47.05	73.91	18.43	0.90	0.30	0.62
L24	0.70	5.00	43.60	54.64	98.16	0.84	0.45	0.18	0.05

\* Obtained from separate calcination tests.

## Results and Discussion

By SEM and elemental analysis of OS it was determined that Ca distribution over the cross-section of the OS sample is compact (Fig. 1), and calcium carbonate is not remarkably dispersed in the organic part. So, modeling of decarbonization and sulphation on the basis of natural limestone would be a suitable approach.

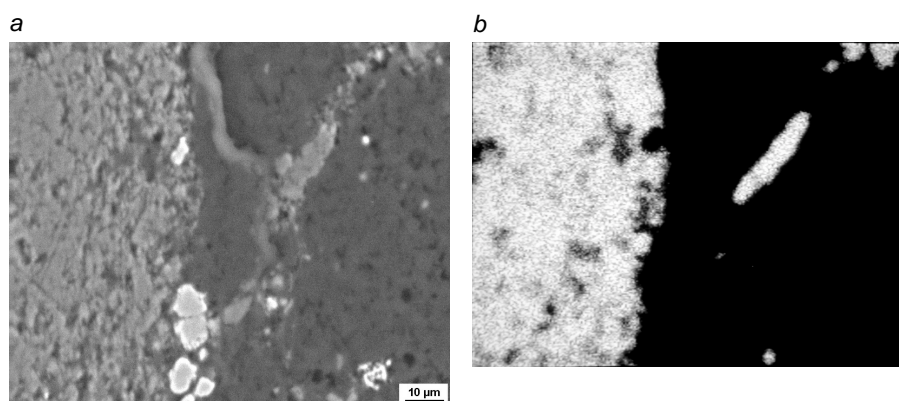


Fig. 1. SEM photo of the cross-section of OS sample (a) and calcium distribution over the cross-section (white areas at b)

## Calcination

During limestone calcination, the specific surface and porosity of the samples studied mainly increased. The increase was the higher, the lower the content of impurities and initial specific surface (see Table 1). Increase in the calcination temperature significantly decreased the specific surface of the lime obtained and led to a significant decrease in porosity. Therefore, as for these samples, the intrusion of SO<sub>2</sub> into the pores should be difficult, and the binding reaction should take place mostly on the surface.

SEM analysis (Fig. 2) showed the formation of particles of high porosity and sponge-like structure when calcinated at lower temperatures, but formation of liquid phase and pore blocking at higher temperatures (over 950 °C). CaO, MgO, quartz and larnite (β-Ca<sub>2</sub>SiO<sub>4</sub>) were the main phases in the calcinated samples.

Mathematically, the calcination process of limestone samples was satisfactorily described using a random pore distribution model, assuming that only chemical reaction limited the overall decomposition process:

$$\frac{dX}{dt} = k_w(T) \cdot F(\text{CO}_2) \cdot S_{\text{CaCO}_3}(X) \cdot \frac{M_{\text{CaCO}_3}}{\rho_{\text{CaCO}_3}} \quad (1)$$

where  $k_w$  is reaction rate constant depending on temperature  $T$  by Arrhenius equation;

$F(\text{CO}_2)$  is factor describing CO<sub>2</sub> partial pressure above the sample calculated from thermodynamic data;

$M_{\text{CaCO}_3}$  is molar mass of CaCO<sub>3</sub>, kg/kmol;

$\rho_{\text{CaCO}_3}$  is density of CaCO<sub>3</sub>, kg/m<sup>3</sup>;

$S_{\text{CaCO}_3}(X)$  is a conversion dependent on CaCO<sub>3</sub> specific surface (m<sup>2</sup>/m<sup>3</sup>), which can be found by

$$S_{\text{CaCO}_3}(X) = S_{v0} \cdot (1 - X) \cdot [1 - \Psi \cdot \ln(1 - X)]^{1/2} \quad (2)$$

where  $S_{v0}$  is pore surface area of raw sorbent particle, m<sup>2</sup>/m<sup>3</sup>;

parameter  $\Psi$  characterises the structure of pores and depends on the initial porosity and pore size distribution [9].

Equation (1) was solved together with the temperature increase equation that gives temperature and the degree of conversion depending on reaction time  $t$  (Fig. 3). Rate constants for limestone decomposition at 780 °C in 15% CO<sub>2</sub> medium were in the range from  $9.7 \cdot 10^{-11}$  to  $2.9 \cdot 10^{-9}$  kmol/(m<sup>2</sup> · s), activation energies calculated from the model by approximation in the range of 260–390 kJ/mol. Since diffusion resistance and heat transfer were not taken into account, the values of  $E_A$  obtained by this method have no strict physical meaning and can be used as comparative characteristics for the samples studied. However, the RP model was satisfactorily used for mathematical description of the process of limestone calcination under dynamic temperature increase conditions.

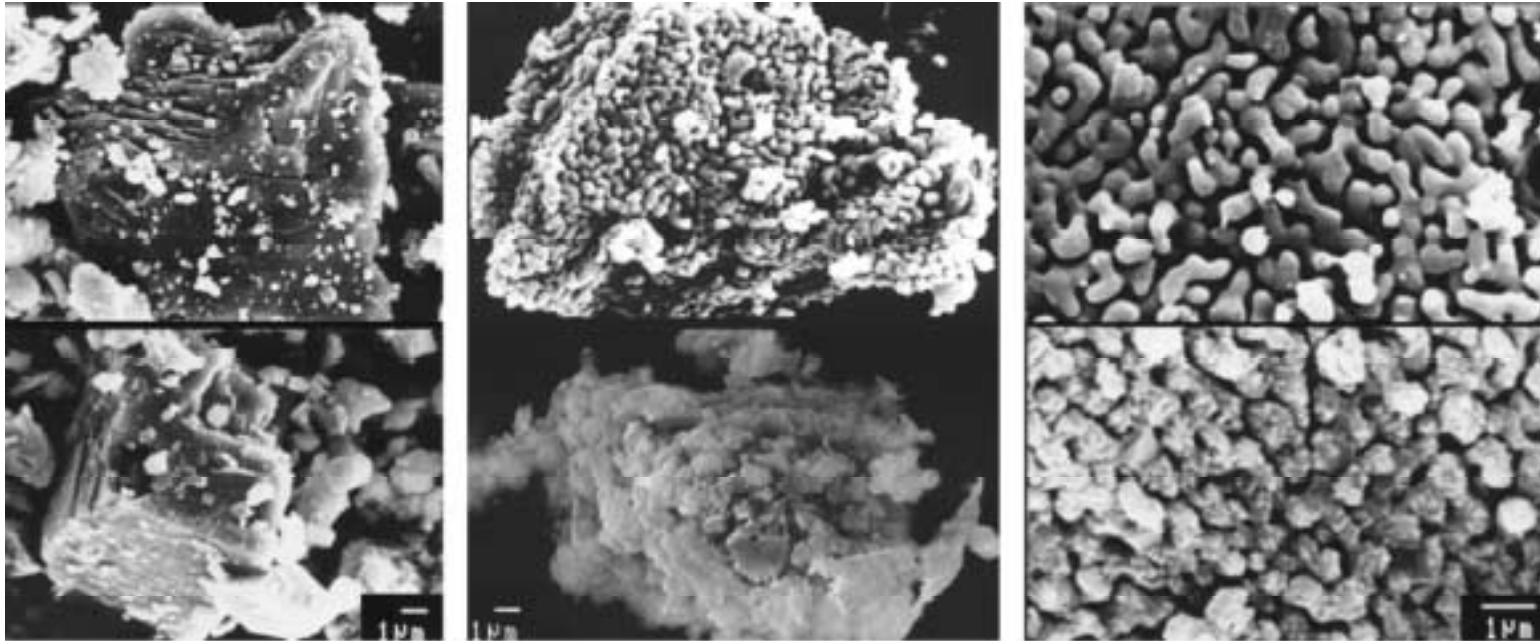


*Fig. 2.* SEM photos of initial limestone samples L24 (left above) and L14 (left below); L24 calcinated at 940 °C (middle above, right above) and 1100 °C (middle below); L24 calcinated at 940 °C and sulphated at 940 °C for 20 min (right below)

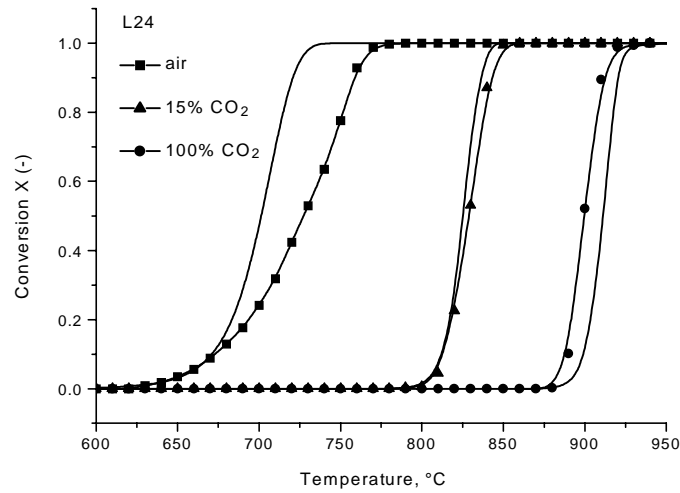


Fig. 3. Comparison of experimental (line with markers) and calculated decarbonization data

### Sulphation

During sulphation, the specific surface and porosity decreased, but the pores were not blocked totally (see Fig. 2).  $\text{SO}_2$  was bound mainly as anhydrite or  $\gamma\text{-CaSO}_4$ .

The conventional USC model was extended with variable (or conversion dependent) effective diffusivity [13–16, 18] and used for modeling sulphation data concerning both atmospheric conditions and elevated pressure.

In the process of sulphur capture four different steps can be distinguished, which can be simultaneously rate determining: external mass transfer, sample-bed diffusion, chemical kinetics and diffusion inside the particle. Besides, the structure of the particle is continuously changing during sulphation. In this case the concept of “additive reaction times” [17] was used. According to this concept and considering necessary corrections for sample-bed diffusion and external mass transfer, the time  $t$  to achieve a certain degree of conversion  $X$  can be found as

$$t = \tau_{kin}F_{kin}(X) + \tau_{dif}F_{dif}(X) \quad (3)$$

where  $t$  is overall reaction time, s;

$\tau_{kin}$ ,  $\tau_{dif}$  are time constants for chemical kinetics and diffusion;  
 $F_{kin}(X)$ ,  $F_{dif}(X)$  are conversion functions describing kinetics and diffusion.

The USC model with variable effective diffusivity is expressed as follows:

$$t = \tau_{kin}F_{kin}(X) + \tau_{dif,0} \frac{1+BX}{1+AX} F_{dif}(X) \quad (4)$$

where  $A$  and  $B$  are dimensionless parameters ( $A$  depending on initial porosity).

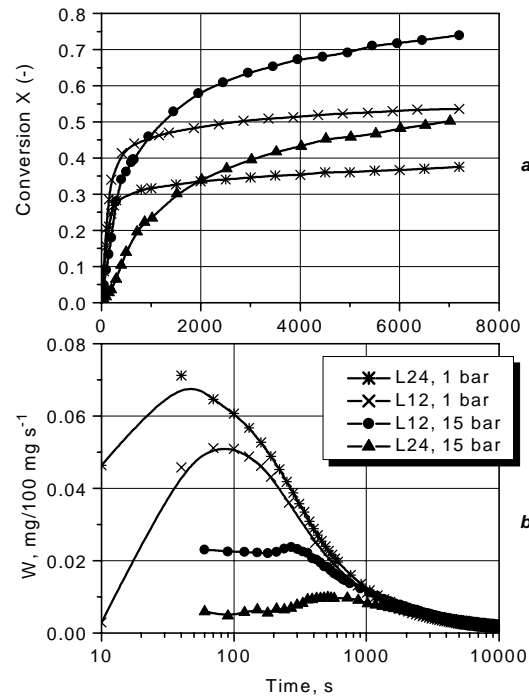


Fig. 4. The effect of pressurising on SO<sub>2</sub> binding properties of two limestone samples: *a* – degree of conversion, *b* – binding rate

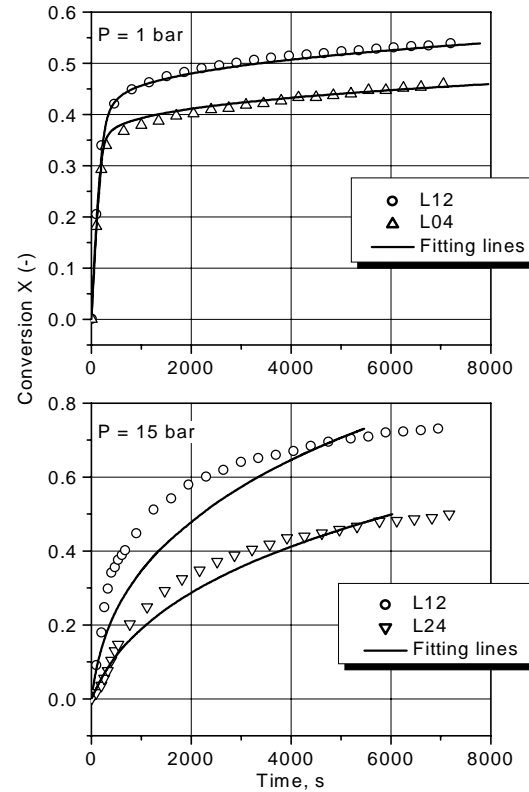


Fig. 5. Comparison of experimental SO<sub>2</sub> binding data (markers) with those calculated by the extended USC model (lines)

Parameters into this model ( $\tau_{dif,0}$  and  $B$ ) were found using a non-linear least squares curve fitting routine, kinetics time constant using a Taylor series expansion of Equation (3) as described earlier by Zevenhoven *et al.* [18]. Having determined the value for parameter  $B$ , it is possible to calculate also the product layer diffusivity  $D_{pl}$ . Comparison of experimental and calculated data is given in Figures 4 and 5.

At atmospheric pressure the sulphation of decarbonized limestone (conversion of CaO to CaSO<sub>4</sub>) started at a remarkable rate (rate constants  $k_s$  30–90 cm/s), and in 200 s the conversion level reached 25–44% without a significant diffusion resistance of the product layer. So, modeling of sulphation at atmospheric pressure was carried out in two steps assuming that initial stadium was controlled by chemical kinetics resistance only, and in the following stadium (starting at the value of conversion level  $X_{II}$ ) the intraparticle diffusion becomes rate-limiting. Under pressure the sulphation of limestone (direct conversion of CaCO<sub>3</sub> to CaSO<sub>4</sub>) started at a noticeably lower speed (rate constants 0.03–7 cm/s), and the shift from chemical kinetics control to diffusion control occurred at much lower values of conversion. Hence, modeling of sulphation at 15 bar pressure was carried out in one step. The results are presented in Table 2. However, in several cases, especially at atmospheric pressure, the external mass transfer limitations were remarkable at the beginning of the experiment due to the extremely high reactivity of the freshly decarbonized limestone, so the obtained values for the rate constants should be treated with a certain caution.

Table 2. Results of Modeling of Limestone Sulphation

Sample	$k_s$ , m/s	$B$	$A$	$\tau_{dif,0}$ , s	$D_{pl}$ , m <sup>2</sup> /s	$X_{II}$
$P = 1$ bar						
L04	0.343	15,900	0.857	348	$1.28 \cdot 10^{-9}$	0.343
L11	(0.501)*	51,300	0.440	986	$7.67 \cdot 10^{-10}$	0.377
L12	0.406	12,500	0.715	246	$1.27 \cdot 10^{-9}$	0.405
L14	(0.552)*	15,600	0.829	306	$2.07 \cdot 10^{-9}$	0.412
L22	0.306	33,000	0.187	646	$1.64 \cdot 10^{-9}$	0.299
L24	0.909	22,700	0.299	445	$8.29 \cdot 10^{-10}$	0.283
$P = 15$ bar						
L04	0.0687	2,990	5.25	56.6	$6.34 \cdot 10^{-10}$	–
L11	0.0354	7,840	7.70	107.5	$3.26 \cdot 10^{-10}$	–
L12	0.0958	2,290	4.28	31.7	$7.40 \cdot 10^{-10}$	–
L14	(6.75)*	2,770	5.87	54.0	$8.61 \cdot 10^{-10}$	–
L22	0.0771	6,900	4.37	137.0	$4.30 \cdot 10^{-10}$	–
L24	0.0259	3,290	2.48	39.4	$8.22 \cdot 10^{-10}$	–

\* High-external mass-transfer limitations.



## Conclusions

1. Taking into consideration the importance of physical characteristics of the solid phase in the heterogeneous gas – solid interactions, porosity and pore size distribution of several limestone samples as well as their changes at decarbonization and sulphation were determined. Chemical reactions and movement of the reaction front inside the particles during sulphation were specified by means of chemical and X-ray analysis.
2. For a more exact assessment of the role of chemical reactions and diffusion during the heterogeneous sulphation reaction, the respective models were used and improved. The calcination process of limestone samples was satisfactorily described using the random pore distribution model. An attempt was made to apply an extended unreacted shrinking core model to the sulphation data concerning both atmospheric conditions and elevated pressure. From model calculations the kinetic parameters of the decomposition and binding reactions and product layer diffusivities were determined.
3. It was shown by SEM and EDS measurements that the carbonaceous part of OS particles is settled compactly and forms discrete units. This enables to expand the conclusions made in the current paper on the basis of limestone also on the OS carbonaceous part.

## REFERENCES

1. Kikas, V. Mineral matter of kukersite oil shale and its utilization // Oil Shale. 1988. Vol. 5, No. 1. P. 15–28 [in Russian].
2. Kikas, V. Composition and binder properties of Estonian kukersite oil shale ash // International Cement-Lime-Gypsum. 1997. Vol. 50, No. 2. P. 112–126 [Distributed by *Eesti Energia AS (Estonian Energy Ltd.)*].
3. Kaljuvee, T., Trikkel, A., Kuusik, R. Reactivity of oil shale ashes towards sulfur dioxide. 1. Activation of high-temperature ashes // Oil Shale. 1997. Vol. 14, No. 3. P. 393–407.
4. Kuusik, R., Kaljuvee, T., Trikkel, A., Arro, H. Reactivity of oil shale ashes towards sulfur dioxide. 2. Low-temperature ashes formed by using CFBC technology // Oil Shale. 1999. Vol. 16, No. 1. P. 51–63.
5. Kuusik, R., Kaljuvee, T., Veskimäe, H., Roundygin, Yu., Keltman, A. Reactivity of oil shale ashes towards sulfur dioxide. 3. Recurrent use of ash for flue gas purification // Oil Shale. 1999. Vol. 16, No. 4. P. 303–313.
6. Levenspiel, O. Chemical Reaction Engineering. – J.Wiley & Sons, New York, 1972.
7. Khinast, J., Krammer, G. F., Brunner, Ch., Staudinger, G. Decomposition of limestone: The influence of CO<sub>2</sub> and particle size on the reaction rate // Chem. Eng. Sci. 1996. Vol. 51, No. 4. P. 623–634.

8. *Murthy, M. S., Harish, B. R., Rajanandam, K. S.* Investigation on the kinetics of thermal decomposition of calcium carbonate // *Chem. Eng. Sci.* 1994. Vol. 49, No. 13. P. 2198–2204.
9. *Bhatia, S. K., Perlmutter, D. D.* A random pore model for fluid-solid reactions: 1. Isothermal, kinetic control // *AIChE Journal*. 1980. Vol. 26, No. 3. P. 379–385.
10. *Bhatia, S. K., Perlmutter, D. D.* The effect of pore structure on fluid-solid reactions: Application to the SO<sub>2</sub> – lime reaction // *AIChE Journal*. 1981. Vol. 27, No. 2. P. 226–234.
11. *Rundygin, Yu., Alfimov, G., Rundygin, A., Maarend, J., Grigoryev, K., Arkhipov, Yu., Kuusik, R.* Possibilities of deeper desulfurization of flue gases by oil shale ash components in different burning technologies // *Oil Shale*. 1997. Vol. 14, No. 2. P. 115–131.
12. *Szekely, J., Evans, J. W.* A structural model for gas-solid reactions with a moving boundary // *Chem. Eng. Sci.* 1970. Vol. 25. P. 1091–1107.
13. *Zevehoven, R., Yrjas, P., Hupa, M.* Sulfur dioxide capture under PFBC conditions: the influence of sorbent particle structure // *Fuel*. 1998. Vol. 77, No. 4. P. 285–292.
14. *Comelis, A., Zevehoven, P., Yrjas, K. P., Hupa, M. M.* Product layer development during sulfation and sulfidation of uncalcined limestone particles at elevated pressures // *Ind. Eng. Chem. Res.* 1998. Vol. 37, No. 7. P. 2639–2646
15. *Trikkel, A., Zevehoven, R., Kuusik, R.* Estonian calcareous rocks as SO<sub>2</sub> sorbents in AFBC and PFBC conditions // 15th Intern. Conf. on Fluidized-Bed Combustion. May 9–13, 1999, Savannah, Georgia, USA. New York: ASME, 1999, ISBN 0-7918-1962-0. Paper No. FBC 99-0032, 18p., on CD-ROM.
16. *Trikkel, A., Zevehoven, R., Kuusik, R.* Modeling SO<sub>2</sub> capture by Estonian limestones and dolomites // *Proc. Estonian Acad. Sci. Chem.* 2000. Vol. 49, No. 1. P. 53–70.
17. *Sohn, H. Y.* The law of additive reaction times in fluid-solid reactions // *Metallurgical Transactions Bulletin*. 1978. Vol. 9B. P. 89–96.
18. *Zevehoven, C. A. P., Yrjas, K. P., Hupa, M. M.* Hydrogen sulfide capture by limestone and dolomite at elevated pressure. 1. Sorbent performance // *Ind. Eng. Chem. Res.* 1996. Vol. 35, No. 3. P. 943–949.